

520 A Code and Further Resources

521 We provide complementary code in the supplementary of the paper. All models were imple-
522 mented in Python using the PyTorch library. The total training computation required for op-
523 timizing all models and baselines presented in this works amounts to roughly 150 hours (wall
524 clock) on a single standard GPU. Visualization and additional material will be uploaded here
525 <https://sites.google.com/view/velap-cori/home>.

526 B Hyperparameters and algorithm details

527 Here we present a description of the hyperparameter used in method used during the training and
528 inference phases.

529 B.1 Model architectures

Table 2: Hyperparameters of the encoder ϕ

Parameter	Value
Batch-norm.	yes
Filters	[32,32,64,64]
Kernels	[4,4,4,4]
Strides	[2,2,2,2]
Activation	LeakyRelu
Dense layers	[256, 128, 32]

Table 3: Hyperparameters of dynamics model h

Parameter	Value
Batch-norm.	yes
Activation	LeakyRelu
Dense layers	[128,128,128,128,32]

Table 4: Hyperparameters of action sampler g (β -VAE)

Parameter	Value
Batch-norm.	yes
Activation	LeakyRelu
Latent dimension	16
β (kl-weight)	0.01
Encoder dense layers	[128,128,128, 2*16]
Decoder dense layers	[128,128,128, d_{action}]

Table 5: Hyperparameters of policy networks π^l and π^g

Parameter	Value
Batch-norm.	yes
Activation	LeakyRelu
Dense layers	[128,128,128, d_{action}]

Table 6: Hyperparameters of critic networks Q_k^l and Q^g

Parameter	Value
Batch-norm.	yes
Activation	LeakyRelu
Dense layers	[128,128,128, 1]

530 **B.2 Training hyperparameters**

Table 7: Hyperparameters during training (model learning)

Parameter	Value
batch size	64
learning rate (all models)	0.0003
c_0	0.2
c_1 (<i>SpiralMaze</i>)	0.001
c_1 (<i>ObstacleMaze</i>)	1.0
c_1 (metaworld tasks)	0.01
c_2	0.001
c_3	0.001
c_3 (expert)	0.5
γ (discount factor)	0.96
$d_{\mathcal{Z}}$	32
T (temperature parameter)	1.0
n_{ens}	3

531 **B.3 Planner and controller hyperparameters**

Table 8: Hyperparameters during inference (planning)

Name	Description	Value
n_{iter}	Number of planner iterations	250 (500 in <i>ButtonWall</i>)
n_{sim}	Number of simulation steps during tree expansion	5 (10 in <i>SpiralMaze</i> , <i>ButtonWall</i> and <i>DrawerButton</i>)
$\tau_{\text{discard}}^{\text{high}}$	Q-value threshold for discarding node if too close to existing nodes in the tree	γ^2
$\tau_{\text{discard}}^{\text{low}}$	Q-value threshold for discarding node if too far from expansion node	$\gamma^{n_{\text{sim}}}$
$\tau_{\text{discard}}^{\text{std}}$	Q-value threshold for discarding node if standard deviation of ensemble prediction is too high	$1.0 - \gamma$
τ_{neigh}	Q-value threshold to determine neighboring nodes	γ^3
τ_{goal}	Q-value threshold to determine goal nodes	γ^1
d_{neigh}	Euclidean distance threshold to determine candidate neighbors	3 x upper 5-percentile of Eucl. distances between encoding of subsequent states

Table 9: Hyperparameters during inference (controller)

Parameter	Description	Value
n_{replan}	Planning frequency	15 (25 in <i>SpiralMaze</i> , <i>ButtonWall</i>)
ϵ_{goal}	Q-threshold to determine vicinity to the goal	γ^5
ϵ_{wp}	Q-threshold for switching to the next waypoint	γ^3

532 B.4 Training of policy and value functions

533 We use TD3-BC [48] as the base offline RL algorithm to train our local and goal policies π^l and π^g ,
534 respectively state-action value functions Q_k^l and Q^g . Within our planning framework Q_k^l takes an
535 important role as it provides us with a distance proxy. To further improve the accuracy of Q_k^l , we
536 use k Q networks (instead of 2 usually used in TD3). During the training update of the Q-network,
537 we then determine the Q-target by taking the minimum value among the predictions given by the
538 ensemble of Q-networks (similar to [49]). The ensemble further allows us to filter out unlikely
539 or out-of-distribution transitions generated during the tree expansion by thresholding the resulting
540 Q-values based on the minimum predicted ensemble value and the standard deviation among the
541 predicted values.

542 Our models π^l and Q_k^l describe goal-reaching navigation policy and state-action value functions
543 which require a set of goal-conditioned reaching experiences for training. Since our original dataset
544 \mathcal{D} might not provide such data, we augment it using data augmentation via hindsight relabeling. In
545 particular, we create a new dataset \mathcal{D}' creating transitions $(z_t, a_t, r_t, z_{t+1}, z^g, \gamma) \in \mathcal{D}'$ based on the
546 existing transitions in \mathcal{D} by relabeling the values of r_t, γ (γ also indicates terminal condition, i.e.
547 $\gamma = 0$) and adding a new goal state z^g . In this regards, we apply a combination of three different
548 relabeling strategies (a) set goal z^g to be next state of the original transitions and set $\gamma = 0$ and
549 $r_t = 1$ (b) sample z^g from the set of future states within the same trajectory and set $\gamma = 0; r_t = 0$
550 (c) sample z^g from another trajectory in the data and $\gamma = 0$ and $r_t = 0$.

551 B.5 Additional details about planning method

552 **Neighbor computation** To determine if a newly sampled node z_{new} is novel, we check its simi-
553 larity to existing nodes in the tree by evaluating the state-action value function. Yet, evaluating the
554 values network for all nodes in the tree results in an enormous computations overhead. Yet, we can
555 significantly reduce this computation by first determining a set of candidate neighbors around z_{new}
556 using the Euclidean metric and a distance threshold d_{neigh} . In practice, we found it useful to define
557 d_{neigh} based on the statistics of Euclidean distances between subsequent states in the dataset (see
558 App. B.3).

559 **Batch processing** The method in Alg. 1 describes an iterative schema for which at every expansion
560 step one new node is generated and evaluated. Yet, some steps can be computed in parallel on
561 a GPU in order to speed up the planning time. For a practical implementation, we therefore suggest
562 to parallelize the tree expansion by sampling multiple expansion nodes at once and generating new
563 nodes by passing batches through the neural network dynamics model. Similarly, we can compute
564 state-action values in batches instead of assessing one new nodes at a time. For discussions about
565 highly-parallelized implementations of classical RRT-like planners, we refer to [58, 59].

566 B.6 Additional details about MPC controller

567 The below Alg. 2 presents the pseudocode for our MPC controller. The function
568 `update_waypoint(z_{curr}, g^*)` determines the next waypoint z_{wp} which we seeks to achieve using
569 our local policy. In particular, we estimate the value between the current state and waypoint and
570 switch to the next element in g^* if the predicted value surpasses a threshold ϵ_{wp} , i.e $Q_{\text{min}}^{\text{curr}, \text{wp}} > \epsilon_{\text{wp}}$.
571 Once the z_{curr} gets close to the goal, we disable planning and determine actions based on π^g . To
572 determine vicinity to the goal, we check if the prediction of the global value function Q^g exceeds a
573 threshold ϵ_{goal} .

Algorithm 2 MPC controller

Given: $s_{\text{init}}, n_{\text{replan}}, n_{\text{max steps}}, \phi, \pi^l$
 $z_{\text{curr}} \leftarrow \phi(s_{\text{init}})$ ▷ Map state to latent encoding
 $i \leftarrow 0$
while goal not achieved and $i < n_{\text{max steps}}$ **do**
 if not $i \bmod n_{\text{replan}}$ **then** ▷ Replan every n_{replan} steps
 Build tree \mathcal{T} rooted at z_{curr} for n_{iter} steps (Alg. 1).
 Determine $g^* = \{z_{\text{curr}}, z_1, \dots, z_n\}$ given \mathcal{T} (Eq. 8)
 end if
 $z_{\text{wp}} \leftarrow \text{update_waypoint}(z_{\text{curr}}, g^*)$ ▷ Update waypoint if close enough
 $a \leftarrow \pi^l(z_{\text{curr}}, z_{\text{wp}})$ ▷ Compute action given policy
 Execute a and update state
 $z_{\text{curr}} \leftarrow \phi(s_{\text{curr}})$
end while

574 **C Evaluation Environments**575 **C.1 Description of block environments**

576 Similar to the evaluation environments in [14], we implement two long-horizon navigation tasks
577 whose underlying state space is relatively low-dimensional in order to facilitate illustration and
578 visual inspect of learned embeddings using dimensionality reduction techniques such as Isomap
579 [60]. For both environments, the a block robot is controlled using velocity commands while it’s
580 position in constrained to a planar surface.

581 **C.1.1 SpiralMaze**

582 To solve this task, the block agent must navigate form the outer end of the spiral-shaped corridor
583 to the inner region (colored in red; see Fig. 2). The maximum allowed number of episode steps is
584 limited to 300. To generate training data, the agent is placed randomly at a collision free position
585 in the workspace and random actions sequences are applied by subsequently adding Gaussian noise
586 an initially sampled random uniform action. For testing, the agent’s position is sampled uniformly
587 within a small region close to the outer end of the spiral-shaped corridor.

588 **C.1.2 ObstacleMaze**

589 In this environment, the agent must navigate towards the upper wall of the workspace (color in
590 red; see Fig. 2). To achieve the goal the agent must take actions around two obstacles which are
591 randomly placed around the center of the workspace at the beginning of each new episode. The
592 maximum allows number of environment steps is set to 100. For testing, the agent is initialized to
593 random configuration close to wall which is opposite to the goal. We used the same random data
594 collection policy as for the *SpiralMaze* task.

595 **C.2 Description of manipulation environments**

596 We adapted and implemented several robot manipulation environments based on the Metaworld [17]
597 robot benchmark tasks. The underlying physics simulator in this regard is Mujoco [61]. To enable
598 visual manipulation, similar to the problems studied in [6], we enable background rendering of RGB
599 images from a static viewpoint. The robot is controlled by commanding desired endeffector and
600 gripper opening displacements resulting in a 4-dimensional action space. While *WindowClose* and
601 *FaucetClose* were with small modifications adapted from the [17], we evaluate two new scenarios
602 *ButtonWall* and *DrawerButton* which were particularly desired to study our method under extreme
603 sparse reward conditions over a long temporal horizon which requires trajectory ”stitching” to find
604 a solution policy.

605 For data collection, we use a suboptimal policies which takes random actions (additive Gaussian
606 noise) most of the time and with a low probability takes an action generated by a scripted expert

607 policy. Table. 10 provides insight about the number of samples and trajectories in the training data
 608 and as well presents the portion of successful actions (reward=1). For all manipulation tasks, we
 609 set the maximum permitted environmental steps at 150, with the exception of the "ButtonWall"
 610 scenario, where we allow up to 250 steps during the evaluation phase.

611 **C.2.1 WindowClose**

612 In order to accomplish this task, the robotic arm must successfully open a window by shifting a
 613 specific handle sideways. We implement environmental variability by randomly determining the x-y
 614 location of the window object in each episode. During the data collection stage, we randomly set
 615 the positioning of the end-effector above the surface of the table. However, we restrict the sampling
 616 of expert actions to areas close to the objective (window handle). This approach is intended to
 617 guarantee that the strategy employed necessitates to "stitch" different trajectories together to reach
 618 the objective and complete the task when starting from states that are farther away. To ensure
 619 challenging planning situations during testing, we initiate the robot at a significant distance away
 620 from the target.

621 **C.2.2 FaucetClose**

622 This task is similar to the *WindowClose* task, but it requires the agent to use its end-effector to close a
 623 faucet instead. In addition, we employ analogous strategies for data gathering and scenario creation
 624 as those used in the *WindowClose* environment.

625 **C.2.3 ButtonWall**

626 In this scenario, the robot's end-effector is required to navigate around a wall structure before press-
 627 ing a button. The wall's location is randomly set at the beginning of each episode. Furthermore,
 628 a height limitation is imposed on the end-effector to ensure that the agent takes a more extended
 629 path around the wall, as opposed to simply elevating the end-effector. The dataset was produced by
 630 either placing the agent in front of the wall, near the button, or far behind the wall. However, expert
 631 samples in the dataset only exist for scenarios when starting closer to the goal. For testing purposes,
 632 the end-effector is sampled within a restricted region behind the wall to increase the planning task's
 633 complexity.

634 **C.2.4 DrawerButton**

635 In this scenario, the agent is tasked to first close a drawer using its end-effector and subsequently
 636 press a button. To train the agent, we develop a dataset by separately collecting trajectories for each
 637 subtask. This approach necessitates the use of a method capable of combining different trajectories
 638 in the data to devise a solution that achieves the overall task goal.

639 **C.3 Composition of training dataset**

640 The table below presents the composition of our training datasets. Each context in this regards,
 641 refers to a new environment initialization (excl. agent) such as the position of obstacles.

Table 10: Composition of training datasets for each environment

Environment	Num. contexts	Traj. per context	Max. traj. length	Successful transitions
<i>SpiralMaze</i>	1	1000	20	0.12 %
<i>ObstacleMaze</i>	250	20	20	0.11 %
<i>WindowClose</i>	200	10	50	0.48 %
<i>ButtonWall</i>	200	10	50	0.16 %
<i>FaucetClose</i>	200	10	50	0.31 %
<i>DrawerButton</i>	150	20	50	0.16 %

642 D Baseline methods

643 To enable a fair comparison between different methods, we use the same underlying representa-
644 tion/encoder ϕ and dynamics model h in the evaluation of all baselines. For assessing the quality
645 and impact of our representation learner, please review the experimental ablation study in App. E.2.

646 D.1 BC and BC (\mathcal{D}^*)

647 Simple behavioral cloning baselines for which we use the same network architecture as our policy
648 networks (see Table 5) and train using a mean-squared error objective. For \mathcal{D}^* we train only on the
649 subset of successful episodes in the dataset. The train both methods for $3 \cdot 10^5$ iterations using a
650 learning rate of $3 \cdot 10^{-4}$ and batches of size 128.

651 D.2 TD3-BC [48]

652 This baselines resembles the underlying global policy π^g used in VELAP. It provides us with an
653 intuition how well pure offline RL performs without adding any planning methods on top.

654 D.3 IQL [54]

655 This method presents a state of the art model-free offline RL baseline which utilizes expectile regres-
656 sion to estimate state-conditional expectiles of the target values in order to avoid querying values of
657 out-of-sample actions during training. The train IQL for $3 \cdot 10^5$ iterations, a learning rate of $3 \cdot 10^{-4}$,
658 batches of size 256 and $\tau = 0.7$ and $\beta = 3.0$.

659 D.4 MPPI

660 We implement a trajectory optimization baseline similar to the model-based planning algorithm
661 introduced in [7]. The method in [7] presents an adaption of MPPI specifically for the online rein-
662 forcement learning setting which seeks to optimize the expected return of sampled trajectories. To
663 estimate the return, a learned model is used to predict the reward for each trajectory node while a
664 learned Q-function predicts the future return beyond the specified planning horizon. Since rewards
665 in our evaluation environments are sparse, a learned model of the environment reward carries guid-
666 ance for the trajectories optimization as most states have 0 reward. Therefore, we adapt the objective
667 in [7] and instead use the accumulated sum of state-action values as the optimization criterion. This
668 type of scoring function in model-based RL has recently been discussed in [62]. To implement this
669 baseline, we utilize the Q-function of TD3-BC. For all environments, we use 1000 samples per iteration,
670 a planning horizon of 50, elite size 64 and 5 iterations. Replanning is done every 5 environment
671 steps.

672 D.5 MBOP [35]

673 MBOP presents an adaptation of MPPI which was particularly designed for the offline RL setting.
674 It generates new candidate trajectories by adding small amount of Gaussian noise to the actions
675 predicted by a behavioral-cloned policy. To evaluate the quality of the rollouts it uses a truncated
676 value function trained on the offline data. Due to the sparse nature of rewards in our experiments, we
677 found that both the behavioral-cloned policies and the truncated value function were insufficient to
678 generated farsighted behaviors that solve our tasks. To accommodate for the long planning horizons,
679 we instead sample action for a TD3-BC policy and use the corresponding Q-functions to score
680 candidate trajectory during the optimization update. For all environments, we use 1000 samples per
681 iteration, a planning horizon of 50, elite size 64, 5 iterations and a β parameter of 0.7. Replanning
682 is done every 5 environment steps.

683 D.6 IRIS [36]

684 IRIS presents an offline RL methods that was desired particularly for sparse reward environments.
685 It uses a hierarchical decomposition of the planning agent into a low-level and a high-level policy.
686 A conditional VAE model is trained on offline trajectory data and predicts a set of suitable subgoals
687 states that are n -step ahead of the current states. The high-level policy is essentially represented
688 by a Q-function which is chooses the highest values subgoal states among the set of generated
689 candidate states. The low-level policy is then used to navigate towards the predicted subgoal. In
690 all experiments we implement IRIS by training an conditional VAE to predict subgoal states at a
691 horizon of 5 and sample a candidate set of size 256. To implement both the low-level and high-level
692 policy, we use TD3-BC as the base RL algorithm.

693 D.7 IRIS (multi-step)

694 We evaluate an extension of IRIS in which we use the state prediction model to generate multi-step
695 rollouts of suitable subgoals. This strategy increases the exploration horizon and allows to choose
696 the best subgoal from a larger and potentially more diverse set of states. It exploration strategy can
697 also be seen as random shooting of coarse subgoal sequences. In all experiments, we generate 256
698 different trajectories using rollouts of length 5 and a conditional generative model to predict states
699 for a horizon of 5. In our evaluation, we found this method to sometimes perform worse than IRIS.
700 We attribute this to the fact that the global policy doesn't align with the capabilities of the local one,
701 which occasionally results in the selection of subgoal states that might not be attainable.

702 E Supplementary Experiments and Analysis

703 E.1 Physical hardware experiments

704 For the real-world validation of our method, we collected 200 episodes of data for the sponge (\sim
705 15000 samples) and 150 episodes of data for the rope manipulation (\sim 15000 samples) tasks. Train-
706 ing data was generated by operating the robot through a gamepad and took less than 1 hour per task.
707 The collected dataset consist largely of suboptimal trajectories. Successful transition (positive re-
708 ward + episode termination) were labeled during data. We form states by stacking three subsequent
709 images taken by a static camera. The results of a comparison against BC, BC (\mathcal{D}^*) and IRIS are
710 presented in Table 11.

Table 11: Results of physical robot experiments (successful episodes)

Environment	BC	BC \mathcal{D}^*	IRIS	VELAP
Sponge	5/20	6/20	6/20	14/20
Rope	0/20	0/20	2/20	8/20

711 **E.2 Ablating the impact of the learned representation**

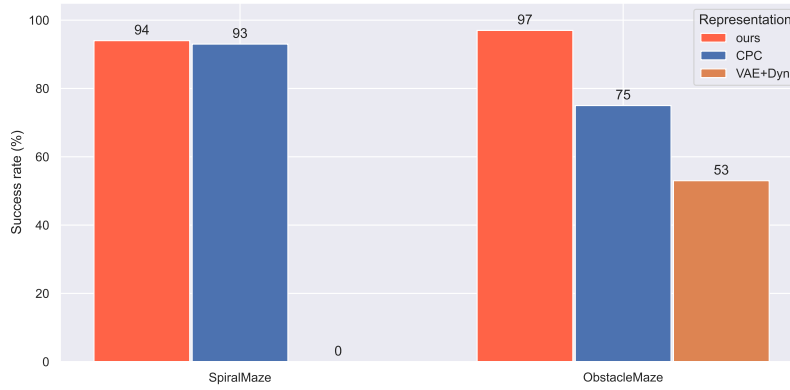


Figure 6: Impact of type of representation on the performance of our planner.

712 **E.3 Influence of the dynamics loss**

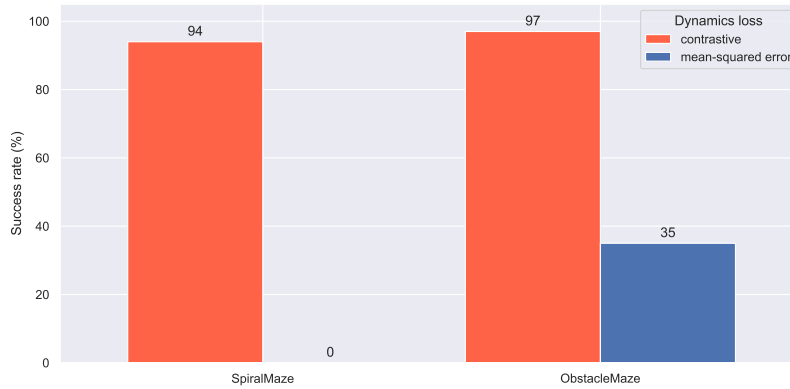


Figure 7: Impact of type of representation on the performance of our planner.